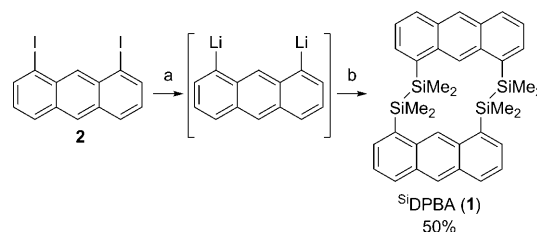


Disilanyl Double-Pillared Bisanthracene: A Bipolar Carrier Transport Material for Organic Light-Emitting Diode Devices**

Waka Nakanishi, Shunpei Hitosugi, Anna Piskareva, Yusuke Shimada, Hideo Taka, Hiroshi Kita, and Hiroyuki Isobe*

The first direct-current electroluminescent material, anthracene, has been the cornerstone molecule for organic electronics.^[1] The first reports on the electroluminescence with single crystals of anthracene demonstrated the potential use of organic molecules as emission materials as well as hole- and electron-transport materials.^[2] Vacuum deposition of anthracene also paved the way for thin-film devices functioning at a low driving voltage (ca. 30 V) albeit at a low quantum efficiency (ca. 0.05 %) and low substrate temperature (ca. –50 °C).^[3] However, the molecule was quickly replaced with aryl amine derivatives for the hole-transport layer (HTL), such as *N,N'*-diphenyl-*N,N'*-bis(1-naphthyl)-1,1'-biphenyl-4,4'-diamine (α -NPD) and with tris(8-hydroxyquinoline)aluminum (Alq₃) for the electron-transport layer (ETL) after the discovery of layered organic light-emitting diodes (OLEDs) with superior performance and stability.^[4,5] Although several derivatives for the emission layer (EML) were accumulated by varying functional groups at the 9- and 10-positions,^[6] the further application of anthracene derivatives as carrier transport materials in layered OLEDs has been rarely explored,^[7] despite the renewed interest in these materials for thin-film organic field-effect transistors (OFETs).^[8] We report herein on the design and synthesis of an anthracene derivative, disilanyl double-pillared bisanthracene (^{Si}DPBA, **1**, Scheme 1), which effectively functions as a bipolar carrier transport material in OLEDs. The device performance using ^{Si}DPBA as both an HTL and ETL material is reasonably high and highlights a new strategy for the molecular design of organic electronic materials.



Scheme 1. Synthesis of ^{Si}DPBA (**1**). a) *t*BuLi (4.0 equiv), THF, –78 °C, 10 min, and room temperature, 10 min. b) ClSiMe₂SiMe₂Cl (1.0 equiv), THF, room temperature, 80 min, 50 % (two steps).

The anthracene derivative ^{Si}DPBA was designed without importing structural motifs established for HTL and ETL materials^[7] and was synthesized in a one-pot procedure from 1,8-diiodoanthracene (**2**; Scheme 1). Thus, **2** was lithiated in the lithium–halogen exchange reaction using *tert*-butyllithium and was subsequently silylated using 1,2-dichlorotetramethyldisilane to give ^{Si}DPBA. Oligomeric byproducts were easily removed by washing with diethyl ether, and the desired compound was obtained in 50 % yield as an analytically pure material without recourse to column chromatography. The product was a single isomer, and the *anti* geometry of the anthracene units was revealed by X-ray crystallographic analysis (see below). We did not detect the other possible isomer with *syn* geometry. The synthesis method is feasible for gram-scale preparation.^[9]

The step-like structure of ^{Si}DPBA was established unequivocally by X-ray diffraction analysis of a single crystal.^[10] As shown in Figure 1a, the antiperiplanar alignment of the C_{ipso}–Si–Si–C_{ipso} moiety positions two adjacent anthracene planes in an antiparallel manner (see also Tables S2 and S3 in the Supporting Information). The torsion angles between the Si–Si single bond and the anthracene plane are in the range 61–73°, which results in a favorable $\sigma_{\text{SiSi}}-\pi$ conjugation (see below).^[11] The molecules are packed with face-to-edge intermolecular contacts similar to unsubstituted anthracene. The arrangement yields a two-dimensional network of intermolecular contacts in the crystal, although the unique step-like shape of the molecule distorts the packing and hinders the formation of typical herringbone motifs (Figure 1b).

Spectroscopic analysis of ^{Si}DPBA revealed favorable properties for the carrier transport materials. The onset absorption wavelength λ_{abs} of ^{Si}DPBA was 401 nm in chloroform (Figure S2 and Table S4 in the Supporting Information), assuring its transparency in most of the visible region. A comparison of the spectrum with that of reference com-

[*] Dr. W. Nakanishi, S. Hitosugi, A. Piskareva, Y. Shimada, Prof. Dr. H. Isobe

Department of Chemistry, Tohoku University
Aoba-ku, Sendai, 980-8578 (Japan)

Fax: (+81) 22-795-6589

E-mail: isobe@m.tohoku.ac.jp

Homepage: <http://www.orgchem2.chem.tohoku.ac.jp/>

Dr. H. Taka, Dr. H. Kita

Display Technology R&D Laboratories

Konica Minolta Technology Center Inc.

2970 Ishikawa-machi, Hachioji-shi, Tokyo 192-8505 (Japan)

[**] This study was partly supported by KAKENHI (21685005, 20108015 to H.I. and 22550094 to W.N.), Nagase Science Technology Foundation, and Konica Minolta Imaging Science Foundation. We thank Emeritus Prof. H. Sakurai (Tohoku Univ.) for helpful discussion, Prof. T. Iwamoto (Tohoku Univ.) for generous discussion and time on X-ray instruments, and JEOL for generous time of DART MS measurement. S.H. thanks the Global COE program (Molecular Complex Chemistry) for a predoctoral fellowship.

Supporting information for this article is available on the WWW under <http://dx.doi.org/10.1002/anie.201002432>.

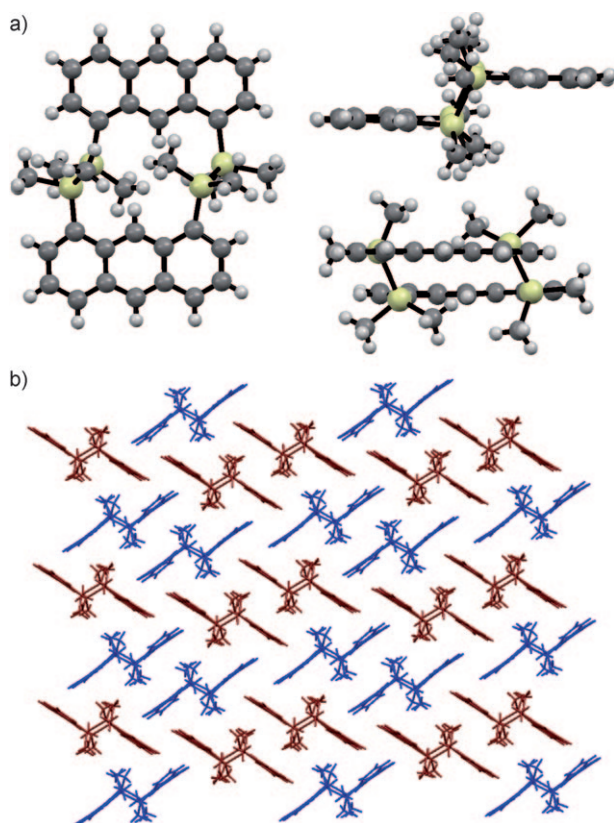


Figure 1. Molecular structures of SiDPBA determined by X-ray crystallographic analysis. a) Ball-and-stick models of SiDPBA viewed perpendicular to the anthracene plane (left) and along the anthracene plane (right). Two inequivalent molecules with similar structures were found in a unit cell, and a representative geometry is shown. C gray, Si yellow, H white. b) Two-dimensional array of SiDPBA in a crystal with intermolecular edge-to-face contacts between neighboring anthracene units. Symmetrically inequivalent molecules are shown in blue and red, respectively.

pounds, such as anthracene ($\lambda_{\text{abs}} = 379 \text{ nm}$) and 1,8-bis(trimethylsilyl)anthracene ($\lambda_{\text{abs}} = 387 \text{ nm}$), confirms the extension of the conjugation through effective $\sigma_{\text{SiSi}}-\pi$ overlap. The onset emission of SiDPBA appeared at 406 nm . The Stokes shift of SiDPBA ($\Delta\lambda = 5 \text{ nm}$) is comparable to that of anthracene ($\Delta\lambda = 7 \text{ nm}$; Figure S3 and Table S4 in the Supporting Information), which indicates the rigidity of the double-pillared structure. We observed neither a $\pi-\pi$ excimer nor a $\sigma_{\text{SiSi}}-\pi^*$ charge-transfer (CT) emission, which have been observed at a longer wavelength with flexible single-tethered bisanthracenes.^[12] The absence of such emissions for SiDPBA may also be ascribed to its structural rigidity and eliminates the possibility of decomposition through the CT process.^[13]

The thermal properties of SiDPBA provide further encouragement for its application in OLED devices. The glass-transition temperature (T_g) was recorded at 153°C using differential scanning calorimetry (DSC). This temperature is higher than those found for standard OLED materials such as α -NPD ($T_g = 100^\circ\text{C}$).^[14] The decomposition temperature (T_d) measured using thermogravimetric analysis (TGA) was also high, at 360°C , with a weight loss of less than 5%.

The device performance of SiDPBA as a carrier transport material was evaluated by employing a standard phosphorescent OLED configuration of ITO (indium tin oxide; 100 nm)/PEDOT:PSS (poly(ethylenedioxy)thiophene:polystyrene sulfonate; 20 nm)/HTL (20 nm)/CBP:[Ir(ppy)₃] ($4,4'$ - N,N' -dicarbazole biphenyl:tris(2-phenylpyridine)iridium; 40 nm)/[hole/exciton blocking layer (HBL; 10 nm)]/ETL (30 nm)/LiF (0.5 nm)/Al (110 nm).^[15] We deposited SiDPBA under vacuum in the HTL, ETL, or both and compared the performance with reference devices containing α -NPD in the HTL and Alq_3 in the ETL. Detailed data of the device evaluation are shown in the Supporting Information (Tables S5 and S6 and Figure S5), and the representative characteristics for the external quantum efficiency (EQE) and the driving voltage are shown in Table 1 as the typical measure of carrier balance and carrier transport ability of the

Table 1: Performance of OLEDs operated at a constant current density of 2.5 mA cm^{-2} .

| Device ^[a] | HTL | HBL | ETL | $V^{[b]}$ [V] | EQE ^[c] [%] |
|-----------------------|-----------------|-----|-----------------|---------------|------------------------|
| A | α -NPD | BCP | Alq_3 | 6.6 | 10.7 |
| B | α -NPD | – | Alq_3 | 7.5 | 3.4 |
| C | α -NPD | – | SiDPBA | 6.7 | 11.0 |
| D | SiDPBA | – | Alq_3 | 8.7 | 3.1 |
| E | SiDPBA | – | SiDPBA | 7.5 | 8.7 |

[a] Device configuration: ITO (100 nm)/PEDOT:PSS (20 nm)/HTL (20 nm)/CBP:[Ir(ppy)₃] (40 nm)/[HBL; 10 nm]/ETL (30 nm)/LiF (0.5 nm)/Al (110 nm). [b] Driving voltage. [c] External quantum efficiency.

new material. A green emission from the phosphorescent guest was observed in all the devices. To maximize the performance, the standard device with α -NPD in HTL and Alq_3 in ETL required bathocuproine (BCP) as HBL (device **A** and **B**), which confirms the hole/exciton leakage into the Alq_3 layer.^[15,16] By confining the hole/triplet in the EML with HBL, device **A** achieved an EQE of 10.7% at a driving voltage of 6.6 V .^[17] When we replaced Alq_3 with SiDPBA , a marked improvement of EQE was achieved in the absence of HBL without raising the driving voltage. Thus, device **C** with SiDPBA in the ETL showed the highest performance, recording the highest external quantum efficiency (EQE = 11.0% at 6.7 V), which is higher than that of the standard devices **A** or **B** with Alq_3 in the ETL (EQE = 10.7 and 3.4%, respectively). Interestingly, device **D** containing SiDPBA in the HTL also showed the green emission with an EQE of 3.1%, which was slightly lower than that of device **B** with α -NPD in the HTL. When we doped SiDPBA in the EML, however, the emission was not detected, which indicates that the material may be able to quench the triplet state of the guest emitter. In turn, the results indicate that the high quantum efficiency of device **C** with SiDPBA in the ETL resulted from an effective electron transport ability that is balanced well with α -NPD. Taking advantage of the bipolar character of SiDPBA , we fabricated device **E** in which SiDPBA was deposited in both the HTL and the ETL and observed the second highest performance (EQE = 8.7% at 7.5 V) in the absence of a HBL.

Theoretical investigations using the DFT method at the B3LYP/6-31G(d,p) level revealed a few key electronic features of ^{Si}DPBA that may contribute to the carrier transport properties.^[18] First, owing to the dimeric anthracene structure, ^{Si}DPBA has pseudo-degenerate frontier orbitals, with neighboring orbitals within a few hundred milli electron volts (HOMO = −5.10 eV, HOMO−1 = −5.28 eV; LUMO = −1.75 eV, LUMO + 1 = −1.63 eV; Figure S7 in the Supporting Information). Second, owing to the participation of σ_{SiSi} and σ^*_{SiSi} orbitals,^[11,19] ^{Si}DPBA possesses a higher HOMO energy and a lower LUMO energy than anthracene (HOMO = −5.24 eV, LUMO = −1.65 eV). The degree of the modulation is moderate to keep the energy gap (3.35 eV) large enough for transparency in the visible-light region.^[20] Furthermore, such a large band gap and a moderate HOMO level may increase the stability toward oxidation.^[21] Third, the combination of $\sigma_{\text{SiSi}}-\pi$ conjugation and the rigid structure results in minimization of the reorganization energy associated with the carrier transport.^[1b] The calculated reorganization energy of ^{Si}DPBA was 105 meV for hole transport and 132 meV for electron transport (Table S7 in the Supporting Information). These values are smaller than those of anthracene (136 meV for hole transport and 202 meV for electron transport),^[22] α -NPD (290 meV for hole transport),^[23] and Alq₃ (260 meV for electron transport)^[24] and rival those of pentacene (100 meV for hole transport and 125 meV for electron transport).^[22] The small reorganization energy of ^{Si}DPBA originates from the delocalization of charge and spin densities without any noticeable structural change in the radical ion species. As shown in Figure 2, the electrostatic surface potentials and spin density of ^{Si}DPBA radical ions are distributed well over the two anthracene units.^[25]

In conclusion, we have designed and synthesized a new anthracene derivative for OLED carrier transport materials. A double-pillaring strategy with disilanyl linkers was successful for the structural and electrical modulation for bipolar materials, which demonstrates that a balanced combination of key players of organic and inorganic (silicon) semiconductors,^[26] a π system and a σ_{SiSi} system, allows delocalization of charge and spin of radical ions over the molecule. A concise route for the pillaring, comprising the substitution reaction of metalated compounds with silylating reagents, should find application in a wide range of aromatic compounds, which may add a new structural repertoire for *n*-type organic semiconductors in particular. Further details of the carrier transport, such as energetics, molecular arrangement in thin films, and the effects of orbital degeneracy, are also interesting from the experimental and theoretical points of view of organic materials.

Received: April 24, 2010

Revised: July 10, 2010

Published online: August 27, 2010

Keywords: acenes · conjugation · cyclophanes · organic semiconducting materials · silylation

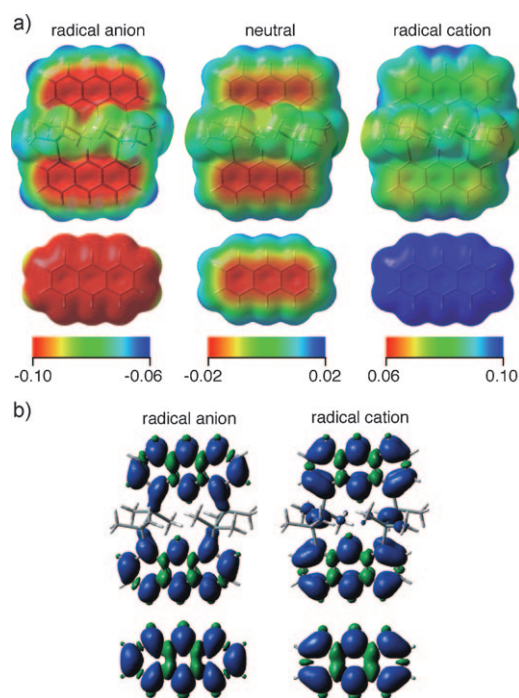


Figure 2. a) Electrostatic surface potentials of ^{Si}DPBA and anthracene mapped onto the surface of total electron density (iso value = 0.0004). Apparent color gradient with ^{Si}DPBA shows a better distribution of charge in the molecule. Regions with higher electron density are shown in red and regions with lower electron density in blue. The color scale bars show the range of potentials with values in atomic units. b) Mulliken atomic spin density surfaces of the radical ions for ^{Si}DPBA and anthracene, showing a better distribution of spin with ^{Si}DPBA. The highest spin density for all the species appeared at the center carbon atoms of the anthracene unit with the following values: ^{Si}DPBA radical anion 0.139, ^{Si}DPBA radical cation 0.130; anthracene radical anion 0.276, anthracene radical cation 0.296.

- [1] a) M. Bendikov, F. Wudl, D. F. Perepichka, *Chem. Rev.* **2004**, *104*, 4891–4945; b) J. L. Brédas, D. Beljonne, V. Coropceanu, J. Cornil, *Chem. Rev.* **2004**, *104*, 4971–5003; c) J. E. Anthony, *Chem. Rev.* **2006**, *106*, 5028–5048; d) J. E. Anthony, *Angew. Chem.* **2008**, *120*, 460–492; *Angew. Chem. Int. Ed.* **2008**, *47*, 452–483.
- [2] a) M. Pope, H. P. Kallmann, P. Magnante, *J. Chem. Phys.* **1963**, *38*, 2042–2043; b) W. Helfrich, W. G. Schneide, *Phys. Rev. Lett.* **1965**, *14*, 229–232; c) W. Mehl, W. Büchner, *Z. Phys. Chem.* **1965**, *47*, 76–88; d) J. Dresner, *RCA Review* **1969**, *30*, 322–334.
- [3] P. S. Vincett, W. A. Barlow, R. A. Hann, G. G. Roberts, *Thin Solid Films* **1982**, *94*, 171–183.
- [4] C. W. Tang, S. A. Vanslyke, *Appl. Phys. Lett.* **1987**, *51*, 913–915.
- [5] a) *Organic Light-Emitting Devices: A Survey* (Ed.: J. Shinar), Springer, New York, **2003**; b) *Organic Light-Emitting Devices: Synthesis, Properties, and Applications* (Eds.: K. Müllen, U. Scherf), Wiley-VCH, Weinheim, **2006**.
- [6] a) Y. H. Kim, D. C. Shin, S. H. Kim, C. H. Ko, H. S. Yu, Y. S. Chae, S. K. Kwon, *Adv. Mater.* **2001**, *13*, 1690–1693; b) J. Shi, C. W. Tang, *Appl. Phys. Lett.* **2002**, *80*, 3201–3203; c) X. H. Zhang, M. W. Liu, O. Y. Wong, C. S. Lee, H. L. Kwong, S. T. Lee, S. K. Wu, *Chem. Phys. Lett.* **2003**, *369*, 478–482; d) Z. L. Zhang, X. Y. Jiang, W. Q. Zhu, X. Y. Zheng, Y. Z. Wu, S. H. Xu, *Synth. Met.* **2003**, *137*, 1141–1142; e) C. A. Landis, S. R. Parkin, J. E. Anthony, *Jpn. J. Appl. Phys.* **2005**, *44*, 3921–3922; f) Y. Y. Lyu, J. Kwak, O. Kwon, S. H. Lee, D. Kim, C. Lee, K. Char, *Adv. Mater.*

- 2008, 20, 2720–2729; g) J. N. Moorthy, P. Venkatakrishnan, P. Natarajan, D. F. Huang, T. J. Chow, *J. Am. Chem. Soc.* **2008**, 130, 17320–17333.
- [7] a) M. X. Yu, J. P. Duan, C. H. Lin, C. H. Cheng, Y. T. Tao, *Chem. Mater.* **2002**, 14, 3958–3963; b) M. A. Reddy, A. Thomas, K. Srinivas, V. J. Rao, K. Bhanuprakash, B. Sridhar, A. Kumar, M. N. Kamalasanan, R. Srivastava, *J. Mater. Chem.* **2009**, 19, 6172–6184.
- [8] a) K. Ito, T. Suzuki, Y. Sakamoto, D. Kubota, Y. Inoue, F. Sato, S. Tokito, *Angew. Chem.* **2003**, 115, 1191–1194; *Angew. Chem. Int. Ed.* **2003**, 42, 1159–1162; b) H. Meng, F. Sun, M. B. Goldfinger, G. D. Jaycox, Z. Li, W. J. Marshall, G. S. Blackman, *J. Am. Chem. Soc.* **2005**, 127, 2406–2407; c) S. Ando, J. Nishida, E. Fujiwara, H. Tada, Y. Inoue, S. Tokito, Y. Yamashita, *Chem. Mater.* **2005**, 17, 1261–1264; d) W. Zhao, Q. Tang, H. S. Chan, J. Xu, K. Y. Lo, Q. Miao, *Chem. Commun.* **2008**, 4324–4326; e) S. Akiyama, S. Misumi, M. Nakagawa, *Bull. Chem. Soc. Jpn.* **1960**, 33, 1293–1298.
- [9] See the Supporting Information for details.
- [10] CCDC 773621 contains the supplementary crystallographic data for this paper. These data can be obtained free of charge from The Cambridge Crystallographic Data Centre via www.ccdc.cam.ac.uk/data_request/cif.
- [11] a) H. Sakurai, M. Kumada, *Bull. Chem. Soc. Jpn.* **1964**, 37, 1894–1895; b) D. N. Hague, R. H. Prince, *Chem. Ind.* **1964**, 1492; c) H. Gilman, W. H. Atwell, G. L. Schwebke, *J. Organomet. Chem.* **1964**, 2, 369–371; d) H. Sakurai, *J. Organomet. Chem.* **1980**, 200, 261–286.
- [12] a) T. Karatsu, T. Shibata, A. Nishigaki, A. Kitamura, Y. Hatanaka, Y. Nishimura, S. Sato, I. Yamazaki, *J. Phys. Chem. B* **2003**, 107, 12184–12191; b) D. D. H. Yang, N. C. C. Yang, I. M. Steele, H. Li, Y. Z. Ma, G. R. Fleming, *J. Am. Chem. Soc.* **2003**, 125, 5107–5110.
- [13] a) M. Kira, T. Miyazawa, H. Sugiyama, M. Yamaguchi, H. Sakurai, *J. Am. Chem. Soc.* **1993**, 115, 3116–3124; b) H. Shizuka, H. Hiratsuka, *Res. Chem. Intermed.* **1992**, 18, 131–182.
- [14] a) S. Yamaguchi, K. Tamao, *Bull. Chem. Soc. Jpn.* **1996**, 69, 2327–2334; b) H. Y. Cho, L. S. Park, Y. S. Han, Y. Kwon, J. Y. Ham, *Mol. Cryst. Liq. Cryst.* **2009**, 499, 323–332.
- [15] a) M. A. Baldo, S. Lamansky, P. E. Burrows, M. E. Thompson, S. R. Forrest, *Appl. Phys. Lett.* **1999**, 75, 4–6; b) *Highly Efficient OLEDs with Phosphorescent Materials* (Ed.: H. Yersin), Wiley, Weinheim, **2008**.
- [16] M. A. Baldo, S. R. Forrest, *Phys. Rev. B* **2000**, 62, 10958–10966.
- [17] The quantum efficiency of reference device **B** without the HBL was also improved from the reported device (reference [15]) probably with the aid of LiF in the electron-injecting layer.
- [18] Gaussian09 (Revision A.02): M. J. Frisch et al., see the Supporting Information.
- [19] M. Shimizu, K. Oda, T. Bando, T. Hiyama, *Chem. Lett.* **2006**, 35, 1022–1023.
- [20] Profound conjugation with sp²/sp pillars between two anthracene units disrupts the transparency. See for example: a) S. Akiyama, M. Nakagawa, *Bull. Chem. Soc. Jpn.* **1971**, 44, 3158–3160; b) S. Toyota, M. Kurokawa, M. Araki, K. Nakamura, T. Iwanaga, *Org. Lett.* **2007**, 9, 3655–3658; see also reference [8].
- [21] H. Meng, Z. Bao, A. J. Lovinger, B. C. Wang, A. M. Muijsce, *J. Am. Chem. Soc.* **2001**, 123, 9214–9215.
- [22] V. Coropceanu, M. Malagoli, D. A. da Silva Filho, N. E. Gruhn, T. G. Bill, J. L. Brédas, *Phys. Rev. Lett.* **2002**, 89, 275503.
- [23] B. C. Lin, C. P. Cheng, Z. P. M. Lao, *J. Phys. Chem. A* **2003**, 107, 5241–5251.
- [24] S. H. Dong, W. L. Wang, S. W. Yin, C. Y. Li, J. Lu, *Synth. Met.* **2009**, 159, 385–390.
- [25] The energy gap between S₀ and T₁ states of ^{si}DPBA (2.3 eV, adiabatic, B3LYP/6-31G(d,p)) is slightly lower than the triplet energy of [Ir(ppy)₃] (2.4 eV).^[16] The result suggests that ^{si}DPBA may not help the confinement of triplets in EML and that the effective electron transport ability contributes largely to the high quantum efficiency. Note, however, that the triplet energy of ^{si}DPBA is much higher than that of anthracene (1.3 eV, reference [15b]). See also P. Marsal, I. Avilov, D. A. da Silva Filho, J. L. Brédas, D. Beljonne, *Chem. Phys. Lett.* **2004**, 392, 521–528.
- [26] R. D. Miller, J. Michl, *Chem. Rev.* **1989**, 89, 1359–1410.